JOURNAL OF
MEDICINAL
CHEMISTRY

© Copyright 1991 by the American Chemical Society

Volume 34, Number 7 July 1991

Perspective

Design of Enzyme Inhibitors Using Iterative Protein Crystallographic Analysis†

Krzysztof Appelt, Russell J. Bacquet, Charlotte A. Bartlett, Carol L. J. Booth, Stephan T. Freer, Mary Ann M. Fuhry, Michael R. Gehring, Steven M. Herrmann, Eleanor F. Howland, Cheryl A. Janson, Terence R. Jones, Chen-Chen Kan, Vinit Kathardekar, Kathleen K. Lewis, Gifford P. Marzoni, David A. Matthews, Christopher Mohr, Ellen W. Moomaw, Catharine A. Morse, Stuart J. Oatley, Richard C. Ogden, Mutyala Rami Reddy, Siegfried H. Reich, Warren S. Schoettlin, Ward W. Smith, Michael D. Varney, J. Ernest Villafranca, Robert W. Ward, Stephanie Webber, Stephen E. Webber, Katherine M. Welsh, and Jennifer White

Agouron Pharmaceuticals, Inc., 11025 North Torrey Pines Road, La Jolla, California 92037. *Received December 18, 1990*

Introduction

From the conceptual breakthrough made by Ehrlich[1] that a drug has a highly specific receptor target at the cellular level to the early work of Hitchings and Roth[2] and Black and colleagues,[3] the development of receptor-based drug design has profoundly benefited the drug discovery process. A historical survey of drug discovery shows that it is possible to improve the pharmacological activity of a "lead" compound by systematic modification of its chemical structure in conjunction with biological and, ultimately, clinical evaluation. Current methods for discovering lead compounds rely both on screening natural and synthetic inventories using a receptor-based or cellular-based assay and on the development of antimetabolites based on knowledge of key biochemical pathways. These strategies yield molecules whose structures must be modified in order to manipulate their activity and toxicity.

Knowledge of the three-dimensional structure of pharmacologically significant receptor–ligand complexes at the level of resolution achieved by X-ray crystallography clearly has the potential for profoundly influencing and speeding the discovery and development of lead compounds. From experimental observations at the atomic level of how inhibitors bind to their macromolecular targets, specific interactions that are important in molecular recognition can be inferred. This knowledge can be widely applied to the de novo design of novel leads as well as to the improvement of existing leads. With a few isolated exceptions, the application of such a strategy has not yet been extensive or systematic enough to define a new methodology. Pioneering work was done by Goodford and colleagues,[4] who used the crystal structure of hemoglobin as a basis for ligand design. This was followed by the studies of Matthews et al.,[5] who carried out a retrospective crystallographic analysis of vertebrate and bacterial dihydrofolate reductase (DHFR) complexed with the highly

Scheme I. An Iterative Cycle for the Discovery and Elaboration of Lead Compounds

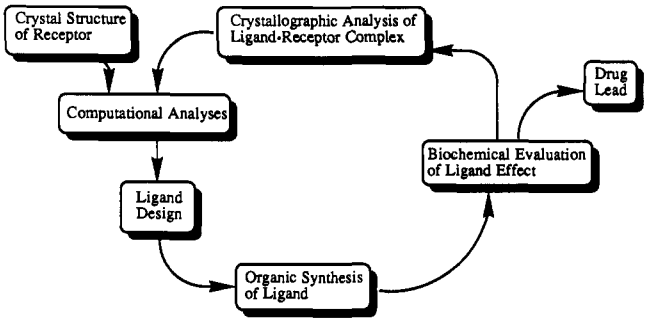

† This paper is dedicated to the memory of our colleague Stuart Oatley.

(1) Ehrlich, P. *Ber. Dtsch. Chem. Ges.* **1909**, *42*, 17.
(2) Hitchings, G. H.; Roth, B. In *Enzyme Inhibitors as Drugs*; Sandler, M., Ed.; University Park Press: Baltimore, MD, 1980; p 263.
(3) (a) Black, J. W.; Duncan, W. A. M.; Durant, G. J.; Ganellin, C. R.; Parsons, M. E. *Nature* **1972**, *236*, 385. (b) Black, J. W.; Stephenson, J. S. *Lancet* **1962**, *2*, 311.
(4) (a) Beddell, C. R.; Goodford, P. J.; Norrington, F. E.; Wilkinson, S.; Wootton, R. *Br. J. Pharmacol.* **1976**, *57*, 201. (b) Brown, F. F.; Goodford, P. J. *Br. J. Pharmacol.* **1977**, *60*, 337. (c) Beddell, C. R.; Goodford, P. J.; Kneen, G.; White, R. D.; Wilkinson, S.; Wootton, R. *Br. J. Pharmacol.* **1984**, *82*, 397.
(5) Matthews, D. A.; Bolin, J. T.; Burridge, J. M.; Filman, D. J.; Volz, K. W.; Kraut, J. *J. Biol. Chem.* **1985**, *260*, 392.

0022-2623/91/1834-1925$02.50/0 © 1991 American Chemical Society

potent drugs methotrexate and trimethoprim and who were able to rationalize the selectivity of the latter. Later, Kuyper et al.[6] used the *E. coli* DHFR structure to design a trimethoprim analogue with increased in vitro activity, and more recently Ripka et al.[7] and Baldwin et al.,[8] among others, have described the increasing influence of the knowledge of receptor structure on the design of ligands. It is now practical to introduce an iterative cycle of design, synthesis, evaluation, and crystallographic analysis into the process of discovery and elaboration of lead compounds for pharmaceutical study (Scheme I). In this paper we demonstrate the application of such a strategy to the *E. coli* enzyme thymidylate synthase (TS, EC 2.1.1.45).

Since the 1970's, the many disciplines that bring specialized knowledge to bear on the study of drug–receptor interaction have undergone great technological and conceptual advances. Recombinant DNA technology has made it possible to isolate genes encoding protein receptors from target organisms and to generate their products in the quantities necessary for a dedicated crystallographic effort. The development of protein chromatography systems has streamlined the isolation of highly purified protein, a prerequisite for crystallization studies. Advances in X-ray crystallographic data collection equipment, computer hardware, and crystallographic applications software have made it possible, in favorable cases, to solve a new protein structure in 1 year or less and to carry out within a few days difference Fourier analyses that compare isomorphous ligand–receptor complexes with the known receptor structure to reveal the details of ligand binding. The development of powerful interactive graphics hardware and its associated molecular modeling software has provided a smooth link between the structure of the complexed ligand and the ongoing ligand-design process. Finally, the increasing sophistication of theoretical and computational methods together with more powerful and less expensive computers has provided insight into ligand conformations, receptor characteristics, and ligand–receptor interactions.

Much has been written about the potential that the interplay of all these disciplines, along with that of medicinal chemistry, could have on the de novo design of potent inhibitors and their elaboration into drugs.[9] In this paper we describe a series of case histories that exemplify both the elaboration of an existing drug lead into a series of new molecules with different properties in cultured cells and the de novo design of structurally diverse and novel lead inhibitors and their development into potent drug leads by iterative crystallographic analysis.

Thymidylate Synthase as a Receptor for X-ray Crystal Structure Based Inhibitor Design

The enzyme thymidylate synthase mediates the methylation of deoxyuridylate to thymidylate using 5,10-methylenetetrahydrofolate as cofactor. This is the rate-limiting step in the de novo pathway to thymidine nucleotides. TS has been the focus of intensive research aimed at generating a novel antifolate antitumor agent with properties superior to those of the clinically established dihydrofolate reductase inhibitor methotrexate.

Classical antifolate TS inhibitors such as compounds **1** and **2** (Table I) have been described in the literature.[10,11] They are characterized by the presence of a glutamate moiety and are generally partially metabolized within the cell to noneffluxable polyglutamate forms.[12] In vitro analyses[13-15] at low ionic strength have shown that polyglutamylated TS inhibitors bind tighter than the corresponding monoglutamylated forms, with K_is, in some cases, in excess of 2 orders of magnitude lower. Additionally, in vitro studies[15] of the dissociation rate of the human TS ternary complex formed by **1** and dUMP revealed a half-life of ca. 3 h. These properties may contribute to the toxicity displayed by this class of molecules toward the host.

Two series of nonclassical antifolate TS inhibitors, lacking the glutamate, have recently been described. With a view to removing the requirement for active transport, a frequent source of drug resistance seen in many classical folate antagonists, and introducing transport by passive diffusion, McNamara et al.[16] synthesized analogues of **1** in which the glutamate was replaced by various electron-withdrawing substituents on the phenyl ring. In vitro IC_{50}s for these compounds against mouse L1210 TS were at least 10-fold higher than for **1** although the best of the series were comparable in inhibiting the growth of cells in culture. A clinically useful lipophilic TS inhibitor does not yet exist and is one focus of our efforts in applying the methodology described in this paper.

One goal of our work is to develop novel anticancer agents, making human TS the natural target for structure-based inhibitor design. At the outset, however, we have found it expedient to begin design studies with thymidylate synthase from *E. coli*. The enzyme was abundantly expressed from the cloned *E. coli* gene, was available in the gram quantities necessary for an intensive, iterative crystallographic effort, and yielded X-ray diffraction quality crystals. Furthermore, the primary sequence of the *E. coli* enzyme has high homology (46% identity) to the human TS sequence.[17] Following determination of the three-dimensional structure of *E. coli* TS in both apo and ternary complex forms,[18,19] it became

(6) Kuyper, L. F.; Roth, B.; Baccanari, D. P.; Ferone, R.; Beddell, C. R.; Champness, J. N.; Stammers, D. K.; Dann, J. G.; Norrington, F. E.; Baker, D. J.; Goodford, P. J. *J. Med. Chem.* **1985**, *28*, 303.
(7) Ripka, W. C.; Sipio, W. J.; Blaney, J. M. *J. Heterocycl. Chem.* **1987**, *24*, S-95.
(8) Baldwin, J. J.; Ponticello, G. S.; Anderson, P. S.; Christy, M. E.; Murcko, M. A.; Randall, W. C.; Schwam, H.; Sugrue, M. F.; Springer, J. P.; Gautheron, P.; Grove, J.; Mallorga, P.; Viader, M.-P.; McKeever, B. M.; Navia, M. A. *J. Med. Chem.* **1989**, *32*, 2510.
(9) (a) Beddell, C. R. *Chem. Soc. Rev.* **1984**, *13*, 279. (b) Hol, W. G. J. *Angew. Chem., Int. Ed. Engl.* **1986**, *25*, 767. (c) Cohen, N. C.; Blaney, J. M.; Humblet, C.; Gund, P.; Barry, D. C. *J. Med. Chem.* **1990**, *33*, 883. (d) Roth, B. *Fed. Proc. Fed. Am. Soc. Exp. Biol.* **1986**, *45*, 2765.
(10) Jones, T. R.; Calvert, A. H.; Jackman, A. L.; Brown, S. J.; Jones, M.; Harrap, K. R. *Eur. J. Cancer* **1981**, *17*, 11.
(11) Hughes, L. R.; Jackman, A. L.; Oldfield, J.; Smith, R. C.; Burrows, K. D.; Marsham, P. R.; Bishop, J. A. M.; Jones, T. R.; O'Connor, B. M.; Calvert, A. H. *J. Med. Chem.* **1990**, *33*, 3060.
(12) Sikora, E.; Jackman, A. L.; Newell, D. R.; Calvert, A. H. *Biochem. Pharmacol.* **1988**, *37*, 4047.
(13) Cheng, Y.-C.; Dutschman, G. E.; Starnes, M. C.; Fisher, M. H.; Nanavathi, N. T.; Nair, M. G. *Cancer Res.* **1985**, *45*, 598.
(14) Pawelczak, K.; Jones, T. R.; Kempny, M.; Jackman, A. L.; Newell, D. R.; Krzyzanowski, L.; Rzeszotarska, B. *J. Med. Chem.* **1989**, *32*, 160.
(15) Pogolotti, A. L.; Danenberg, P. V.; Santi, D. V. *J. Med. Chem.* **1986**, *29*, 478.
(16) McNamara, D. J.; Berman, E. M.; Fry, D. W.; Werbel, L. M. *J. Med. Chem.* **1990**, *33*, 2045.
(17) Hardy, L. W.; Finer-Moore, J. S.; Montfort, W. R.; Jones, M. O.; Santi, D. V.; Stroud, R. M. *Science*, **1987**, *235*, 448.
(18) (a) Matthews, D. A.; Appelt, K.; Oatley, S. J.; Xuong, Ng. H. *J. Mol. Biol.* **1990**, *214*, 923. (b) Matthews, D. A.; Villafranca, J. E.; Janson, C. A.; Smith, W. W.; Welsh, K.; Freer, S. *J. Mol. Biol.* **1990**, *214*, 937.

Table I. Structures and in Vitro Inhibition Constants of Inhibitors

no.	substituent	K_i,[a] μM		IC_{50},[b] μM		
		E. coli TS	human TS	L1210	CCRF-CEM	GC_3/M TK$^-$
	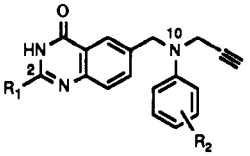					
1	$R_1 = NH_2$, R_2 = *p*-COGlu	0.0030 ± 0.0003 0.0053 ± 0.0020	0.012 ± 0.003 0.010 ± 0.003	3.5	0.75	1.4
2	$R_1 = CH_3$, R_2 = *p*-COGlu	0.0048 ± 0.0011 0.013 ± 0.003	0.0085 ± 0.0044 0.0078 ± 0.0033	0.059	0.043	0.049
3	$R_1 = CH_3$, $R_2 = H$	4.0 ± 1.2 15 ± 7	2.2 ± 1.6 5.7 ± 1.9	>10.7 (35%)[c]	>10.7 (30%)[c]	>10.7 (25%)[c]
4	$R_1 = CH_3$, R_2 = *m*-CF_3	0.45 ± 0.21 2.2 ± 0.8	0.39 ± 0.14 >4.3 (35%)	>4.3 (35%)[c]	>4.3 (40%)[c]	>4.3 (35%)[c]
5	$R_1 = CH_3$, R_2 = *p*-SO_2Ph	0.025 ± 0.006 0.067 ± 0.048	0.013 ± 0.006 0.023 ± 0.010	1.0	1.6	1.1
6	$R_1 = CH_3$, R_2 = *m*-CF_3, *p*-SO_2Ph	0.037 ± 0.020 0.040 ± 0.008	0.050 ± 0.031 0.084 ± 0.002	2.0	3.5	7.5
7	$R_1 = CH_3$, R_2 = *p*-SO_2- 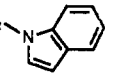	0.15 ± 0.09 0.19 ± 0.10	0.069 ± 0.029 0.062 ± 0.032	0.3	1.3	1.5
	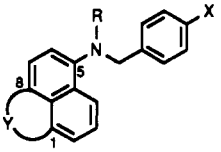					
8	R = C_2H_5, X = SO_2- 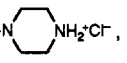 , Y = 	38 ± 31[d] 36 ± 18	3.0 ± 1.0 1.6 ± 0.7	6.0	4.1	16.0
9	R = CH_3, X = SO_2- 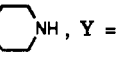 , Y = 	21 ± 11 29 ± 9	0.84 ± 0.32 0.52 ± 0.19	2.3	8.3	25.0
10	R = CH_3, X = SO_2Ph, Y = 	$K_i > 1$[e]	0.77 ± 0.20 0.58 ± 0.34	4.2	3.5	>5 (20%)[c]
11	R = CH_3, X = SO_2Ph, Y = 	1.5 ± 0.5 3.2 ± 1.8	0.031 ± 0.009 0.030 ± 0.013	0.38	1.6	4.6
	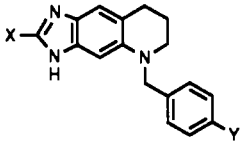					
12	X = H, Y = SO_2- 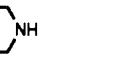	4.9 ± 0.5 34 ± 16	7.7 ± 1.5 11 ± 4.5	20.0	11.0	43.0
13	X = NH_2, Y = SO_2- 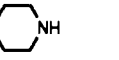	0.14 ± 0.04 1.2 ± 0.6	0.064 ± 0.026 0.12 ± 0.04	2.05	2.2	>50.0 (35%)[c]
14	X = NH_2, Y = SO_2Ph	0.043 ± 0.002 0.48 ± 0.18	0.031 ± 0.003 0.043 ± 0.007	2.0	3.9	>5.0 (25%)[c]

[a] TS activity was assayed by the tritium release method of Lomax and Greenberg[32] with some modifications. Inhibition constants K_{is} (first) and K_{ii} (second) were as described by Cleland,[33] and values listed are averaged over multiple data sets. K_{is} values will be cited in the text. Data were fitted by a nonlinear regression data analysis program.[34] Inhibition patterns were observed to be mixed noncompetitive[35] with respect to CH_2-H_4 folate. While compound 1 has been reported by others[10,15,36] to be a competitive inhibitor with respect to CH_2-H_4 folate, it has been observed by Cheng et al.[13] that the inhibition patterns have never been published and that they do not observe competitive inhibition. [b] Inhibition of cellular growth was measured with a modification[37] of the MTT[38] colorimetric assay of Mosmann[39] using three cell lines, the mouse (L1210) and human (CCRF-CEM) leukemias (ATCC) and a human adenocarcinoma (GC_3/M TK$^-$) deficient in thymidine kinase kindly supplied by Dr. P. J. Houghton and Dr. J. A. Houghton, St. Jude Children's Research Hospital, Memphis, TN. Cells were seeded at 1500 (L1210) or 10 000 (CCRF-CEM, GC_3/M TK$^-$) cells per well in 96-well plates and growth monitored over a range of nine 2-fold serial dilutions of the test compounds in RPMI-1640 culture medium containing 0.5% DMSO. Following a 3 day (L1210) or 5 day (CCRF-CEM, GC_3/M TK$^-$) incubation at 37 °C, cells were harvested after a 4-h treatment with MTT, and growth was measured spectrophotometrically by dissolution of the deposited formazan in DMSO. IC_{50} values were determined from semilogarithmic plots of compound concentration against the mean of the four growth assessments made at each level of the agent relative to the growth of control cultures. [c] Concentrations above this level could not be tested because of insolubility. The figure in parentheses indicates the extent of inhibition at this maximum concentration. [d] Data could only be obtained with a maximum inhibitor concentration at half the K_i and the resultant inhibition constant represents an extrapolated value. [e] The insolubility of the inhibitory compound prevented any value from being determined.

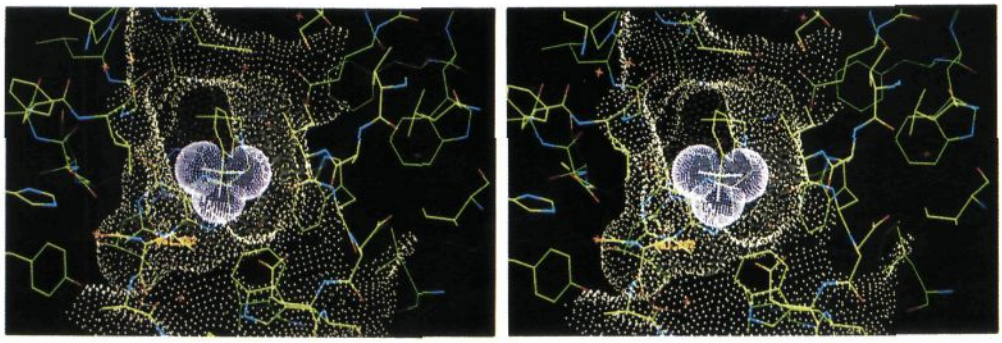

Figure 1. Stereo drawing showing the structure of **4** complexed with *E. coli* TS. All crystals described in this work were grown in space group $P6_1$ as described previously.[18] Protein and ligand atoms are shown in green (carbon), blue (nitrogen), and red (oxygen). Water molecules are represented as red crosses. The solvent-accessible surface of the protein[40] is represented in yellow and the purple spheres represent van der Waals surfaces of the fluorine atoms, shown also in purple. The C_α of Val262 is labeled.

evident that many of the active site residues in the *E. coli* enzyme that form the folate binding site are conserved in the human enzyme (75% identity). Thus it seemed reasonable that the *E. coli* ternary complex structure could serve as a surrogate receptor for the iterative design of human TS inhibitors until the human TS structure was determined. We have, in addition, generated several series of multiple mutants of *E. coli* TS designed to mimic the human enzyme in the active site region.[20] In common with the *E. coli* enzyme, these mutants yielded X-ray diffraction quality crystals. The structures of the mutant enzymes may also provide an experimental view of the ligand binding site in human TS and give some indication of how the human residues, Asn112 (Trp83 in *E. coli*) and Met311 (Val262 in *E. coli*) in particular, interact with a ligand. As an integral part of this work, human TS was expressed in *E. coli* from cDNA (a kind gift from T. Seno) cloned into a dicistronic expression vector. This strategy led to the preparation of ~15 mg of pure, enzymatically active human TS per liter of induced culture. Diffraction data to 3-Å resolution on a ternary complex of human TS containing 5′-fluorodeoxyuridylate and an antifolate inhibitor has been collected and is currently being analyzed.[21]

Structure-Based Elaboration of an Existing TS Inhibitor

As a necessary first step toward increasing the lipophilicity of the water-soluble drug lead 2-methyl-2-desamino-N^{10}-propargyl-5,8-dideazafolic acid (**2**, K_i = 8 nM, human TS), we synthesized analogue **3** (Table I), which lacks the CO-glutamate residue. Compound **3** has a K_i of 2.2 μM and the task was to recoup the 2.4 orders of magnitude of lost binding by substituting lipophilic groups onto the phenyl ring. Examination of the crystal structure of CB3717 (**1**), the closely related 2-amino analogue of **2**, bound to TS showed a small hydrophobic pocket off the meta position of the phenyl ring. Compound **4** (Table I) with a *m*-trifluoromethyl substituent was thus modeled, synthesized, and found to show improved inhibition of both the *E. coli* and human enzymes (Table I). The crystal structure of **4** complexed with *E. coli* TS was solved and, as shown in Figure 1, the trifluoromethyl group occupies the modeled position and makes contact with the side chain of Val262. We next found that a strong electron-withdrawing substituent, such as cyano, at the para position, alone or combined with the *m*-CF_3 substituent, dramatically improved TS inhibition relative to that of **3** or **4**, respectively (at least 10-fold in vitro against *E. coli* TS, data not shown). Simple calculations indicate a better electrostatic interaction with the protein in these cases although dispersion forces and desolvation costs also contribute to the observed binding trend.

The proximity of two hydrophobic side chains, Phe176 and Ile79, to the ligand binding site suggested the possibility that some additional binding energy might be obtained by positioning a large hydrophobic group off the para position of the phenyl group of the lead compound **3**. Consequently, as a way to combine hydrophobicity with electron withdrawal, a *p*-phenylsulfonyl group was modeled. A semiempirical molecular orbital study was conducted to investigate low-energy conformations of the diphenyl sulfone moiety in vacuo. The lack of AM1[22] parameters for sulfur necessitated work initially with a mixed AM1/MNDO or a pure MNDO method[23] for sulfur-containing molecules.[24] These studies of ring rotation in a simplified model of the phenylsulfonyl derivative **5** (Table I) indicated a minimum-energy conformation in which both oxygens are on the same side of each phenyl ring plane. Bisection of the two oxygens by one phenyl ring plane corresponds to the top of a 2–3 kcal/mol barrier. An energy curve computed at this level of theory for an isolated molecule is only a rough guide to actual behavior in an aqueous environment. Nevertheless, it was encouraging that the predicted conformation would place the distal phenyl ring such that it would make the desired nonpolar interaction with the side chain of Ile79. This calculated minimum-energy conformation and the modeled interaction with Ile79 were, in fact, subsequently observed crystallographically (Figure 2). Sulfone **5** was a potent inhibitor of both *E. coli* and human TS with K_is of 25 and 13 nM, respectively.

Compound **6** (Table I), which contains both the trifluoromethyl group and the phenylsulfonyl group, was next examined. Semiempirical calculations showed that introduction of a CF_3 substituent ortho to the sulfone did not change the conformational preference of the phenylsulfonyl substituent. We therefore expected that **6** would inhibit *E. coli* TS better than **5**. No enhanced binding was

(19) (a) Montfort, W. R.; Perry, K. M.; Fauman, E. B.; Finer-Moore, J. S.; Maley, G. F.; Hardy, L.; Maley, F.; Stroud, R. M. *Biochemistry* **1990**, *29*, 6964. (b) Finer-Moore, J. S.; Montfort, W. R.; Stroud, R. M. *Biochemistry* **1990**, *29*, 6977.
(20) Villafranca, J. E.; Foster, P.; Condon, B., unpublished results.
(21) Jordan, S.; Ferre, R.; Booth, C. L. J.; Welsh, K. M., unpublished results.
(22) Dewar, M. J. S.; Zoebisch, E. G.; Healy, E. F.; Stewart, J. J. P. *J. Am. Chem. Soc.* **1985**, *107*, 3902.
(23) Dewar, M. J. S.; Thiel, W. *J. Am. Chem. Soc.* **1977**, *99*, 4899.
(24) Later work with the PM3 method (Stewart, J. J. P. *J. Comput. Chem.* **1989**, *10*, 209.) and with recently developed AM1 sulfur parameters (Dewar, M. J. S.; Yuan, Y.-C., personal communication) agrees closely with the original results.

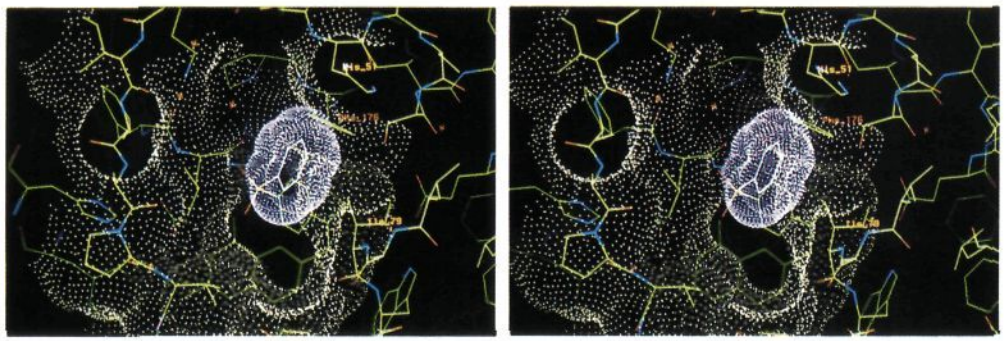

Figure 2. Stereo drawing showing the structure of **5** complexed with *E. coli* TS. Atom colors and surfaces are as described previously with the addition of yellow (sulfur). The distal phenyl group is highlighted in purple and surfaced at the van der Waals radius to illustrate the interaction with the solvent accessible surface created by the side chains of residues His51 and Ile79. The side chain of Phe176 is also labeled.

observed however for either the *E. coli* or the human protein. When the structure of **6** in *E. coli* TS was solved, it became apparent that relative to **5**, accommodation of the CF_3 group required a displacement of the entire diphenyl sulfone moiety and the distal phenyl ring toward Phe176 and His51.

The potency of the *p*-phenylsulfonyl group in this series focused our attention on additional ways to pick up binding energy in this area of the active site. In addition, because of the proximity of this region to bulk solvent, we reasoned that any portion of an inhibitor beyond the distal phenyl group could be designed primarily to address the pharmacological properties of drug leads in this series without significantly affecting binding. The distal phenyl group in **5** was replaced by an indole in compound **7** (Table I). Calculations suggested a very similar low-energy conformation to that of diphenyl sulfone **5** and when modeled in that conformation, favorable nonpolar interactions with Ile79 and His51 were possible. In addition, the SO_2-N linkage provides easier synthetic access to a large number of variants. The K_is of compound **7** against *E. coli* and human TS were found to be 150 and 69 nM, respectively. The crystal structure of **7** and related compounds complexed with *E. coli* TS were solved and are currently being used for subsequent design.

Inhibition of cellular growth was noted for compounds **3–7** (Table I) and was significant for compounds **5–7**. The reduced potency of **6** followed the reduced activity of this compound against the human enzyme. The effects of compounds **5–7** could be reversed by the addition of 10 μM thymidine to the tissue culture media, suggesting that these derivatives exert their effect by the inhibition of intracellular TS.

De Novo Design of Novel TS Inhibitors

In addition to developing existing leads, protein structure-based drug design also makes possible the design of novel leads. For our general purposes, the working definition of a novel lead is a distinct class of compound that (i) has a K_i less than 10 μM, (ii) provides a crystalline complex with protein, and (iii) has a number of positions suitable for elaboration during the iterative cycle shown in Scheme I. The design of novel lead compounds represents the greatest divergence of the structure-based methodology from classical drug-discovery programs. Instead of screening thousands of compounds and biological extracts for a lead which can then be elaborated by either structure–activity relationship (SAR) methodology or the structure-based method described above, de novo design starts with the structure of the receptor.

In this work, design began with a model of the *E. coli* TS ternary complex from which **1** had been removed but in which 5-fluorodeoxyuridylate remained covalently bound. It is crucial to make the distinction between the structure of an uncomplexed receptor and that of a model of the inhibited receptor from which the ligand has been removed. In the latter, it is assumed that the structure of the protein will accurately reflect any conformational changes that result from ligand binding. In the case of TS, such structural accommodations are known to be extensive. The crystal structure of the uncomplexed *E. coli* TS has also been solved[18] and structural comparisons with various ternary complexes indicate that the C terminal tetrapeptide, forming one edge of the active site, moves substantially upon ligand binding. Although the resulting model will, to some extent, and particularly with regard to water molecules and certain side chain conformations, be biased by the structure of the removed ligand, it still provides the most realistic representation of the binding site in its inhibited form.

An important strategic consideration to include in the design of novel leads is to make the compounds sufficiently water soluble so that protein cocrystals can be obtained. This is particularly important with new structural classes of molecules because it is impossible to predict the binding constants in advance, and to facilitate crystallization, the solubility should be approximately equal to or greater than the binding constant. In practice, this is achieved by attaching appropriate polar or charged functional groups to the compounds at positions not expected, from knowledge of the receptor structure, to adversely affect binding. When, in subsequent generations of the lead, the K_i improves significantly, the solubilizing group may be replaced with a group that provides enhanced binding or in vivo potency.

(a) Development of Naphthostyril-Based Lead Compounds. The design of a novel moiety to occupy the pteridine binding site was initiated by running the program GRID[25] with a number of functional group probes. The program, developed by Goodford and colleagues, computes the interaction energies between a functional group probe (e.g. hydroxyl, amino, methyl) and a protein of known structure. The combined electrostatic, hydrogen-bond, and Lennard-Jones energies are represented as equipotential surfaces and displayed along with the protein structure on a computer graphics terminal. Within the *E. coli* active site region, a site interacting favorably with an aromatic CH probe was found and an aromatic ring system (naphthalene) was positioned in that site. Onto this scaffold, a carbonyl group was added at the 1-position to accept a hydrogen bond from an ordered solvent molecule (water

(25) Goodford, P. J. *J. Med. Chem.* **1985**, *28*, 849.

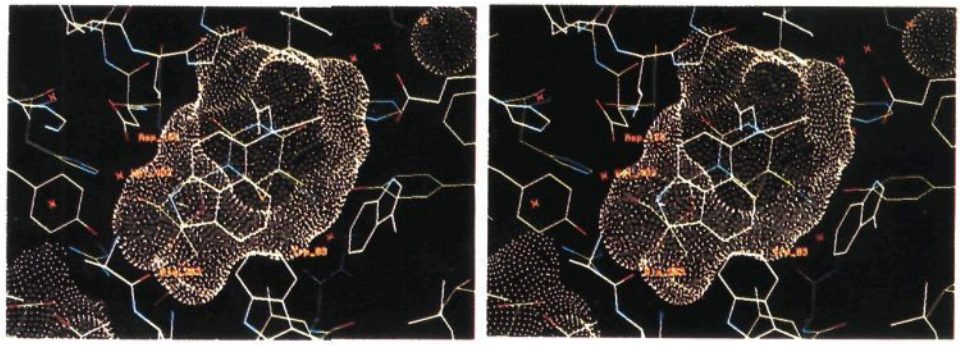

Figure 3. Stereo drawing showing the structure of 8 complexed with *E. coli* TS. The tricyclic portion of the inhibitor is shown and the principle points of contact with the active site residues labeled.

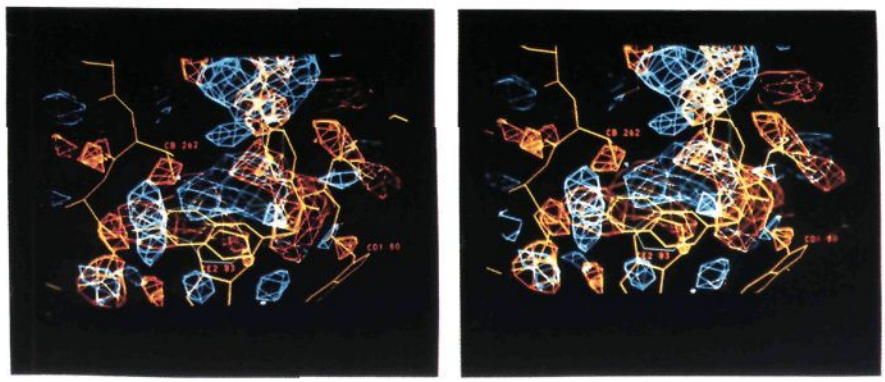

Figure 4. Stereo drawing displaying a portion of the 2.5-Å resolution X-ray difference map between ternary complexes containing respectively compounds 8 (in green) and 1 (in yellow) contoured at -3σ (orange) and $+3\sigma$ (blue). Protein coordinates are those for the refined 2.3-Å ternary complex structure containing 1.[18] The loss of water 430 (a yellow cross within negative (orange) density) and the movement of the backbone carbonyl of Ala263 (negative and positive density apparent) are clearly evident in the lower left of the figure.

430) located at one edge of the TS active site near the protein C terminal tail. An NH group was added at the 8-position to donate a hydrogen bond to the side chain carboxyl of Asp169—an interaction also thought to contribute to binding in the previous series. Both interactions could be made by bridging the 1- and 8-positions with a γ-lactam. The resulting tricyclic ring system, naphthostyril, is commercially available and chemically versatile and thus represented a promising novel substructure. Access to the site occupied by the benzene ring in both folic acid and the previous series of compounds was most plausible from the 5-position of the naphthostyril. Nitrogen was chosen as the linking atom both to avoid the synthetic complication of a chiral center and because a variety of tertiary amines are readily made by alkylation. Ethyl and benzyl substituents for the nitrogen atom were selected for the initial compound based upon their optimum space-filling properties in the modeled conformation. At the para position of the benzyl group, a piperazine ring, for water solubility, was linked through a sulfone group. The (phenylsulfonyl)piperazine moiety had been shown when extending the previous series (**3–7**) to confer both binding and solubility advantages. When modeled, this moiety did not completely superimpose on the experimentally determined binding conformation found in that series, but it was nevertheless judged to be a suitable module for this series. Calculations indicated that the proposed binding conformation was one of two possible low-energy conformations for the molecule.

Compound 8 (Table I) was synthesized and tested for inhibition against both human and *E. coli* thymidylate synthase. The K_is were 3.0 and 38 μM, respectively. Following crystallization of the compound with *E. coli* TS, the binding mode was experimentally determined. Figure 3 shows the tricyclic portion of 8 bound in the active site of *E. coli* TS. The proximity of the ligand to the side chain of Trp83 and the backbone carbonyl of Ala263 is apparent. The ring nitrogen is, however, too far from Asp169 (3.3-Å) to donate a hydrogen bond but may donate a hydrogen bond to a suitably oriented water 402, which itself is bonded to Asp169. The substantial differences between the structures of 1 and 8 complexed with *E. coli* TS are revealed in Figure 4. The positions for the two ligands at the TS active site are superimposed on a difference map to show both the structural differences between the two ligands themselves and the conformational differences induced in the protein when 1 is replaced by 8. Among the more prominent structural changes on going from the ternary complex with 1 to that with 8 is the loss of water 430 and a slight coordinated movement of the terminal carboxylate toward the vacated solvent position. A small upward displacement of the 4-oxo group of FdUMP is coupled with movement of the side chain of Glu58 to which it is hydrogen bonded, and in addition, some side-chain disordering and/or movement for residues in a series of tight turns at one edge of the active site (principally Ile79 and Glu82) is observed. There is also a rotation of the backbone carbonyl of Ala263 away from the lactam carbonyl of 8 to relieve a close nonbonded contact.

The greatest difference between the proposed and observed binding modes for 8 was in the region of the lactam group which is illustrated in Figure 5. The intent behind the modeling was to position the tricyclic ring system (in yellow) so that the lactam group could donate a hydrogen bond to Asp169 (2.9 Å) and accept a hydrogen bond from water 430 (2.8 Å). A close contact between the lactam

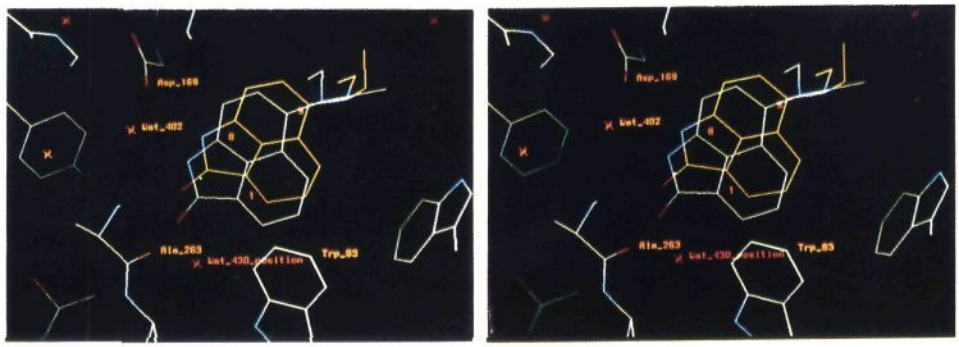

Figure 5. Stereo drawing showing the tricyclic portion of compound **8** modeled (in yellow) and bound (in green) in the active site of *E. coli* TS. The naphthostyril ring numbering system is indicated on the bound structure.

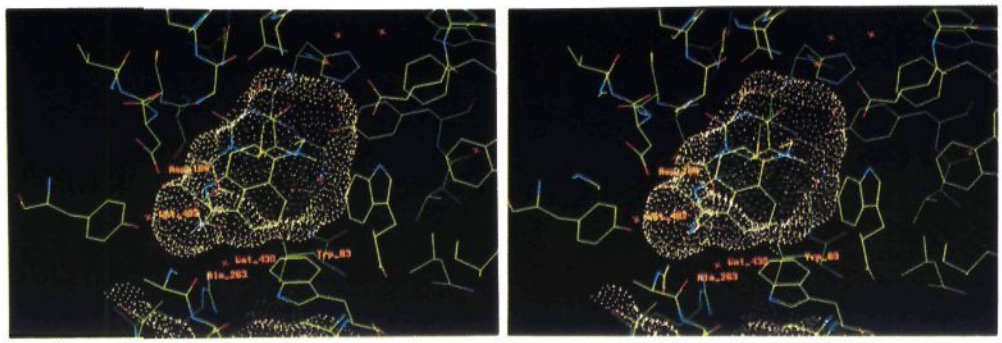

Figure 6. Stereo drawing showing the crystal structure of **11** complexed with *E. coli* TS. The restoration of inferred hydrogen-bonding interactions between the ligand ring and exocyclic nitrogen atoms, protein atoms, and water molecules is shown for the tricyclic portion of **11**.

oxygen and the backbone carbonyl of Ala263 (distance 3 Å) was expected, but it was anticipated that a slight adjustment to the position of the flexible C terminus, including Ala263, would be possible. The ligand was found, however, to bind as indicated in the standard atom colors (Figure 5), displacing water 430 and moving away from Asp169. No immediate explanation for this result was apparent, but the combination of deleterious factors is reflected in the high K_i against the *E. coli* enzyme (Table I). Detailed inspection of the structure suggested that the two principal regions for improvement of the inhibitor were the *N*-9-ethyl substituent and the lactam ring. In the first series of compounds, a variety of N-9-substituents were investigated with the methyl analogue (**9**, Table I) providing the greatest improvement, a factor of 3 against human TS in vitro. The small difference may be due to a more favorable nonpolar interaction with the side chain of Trp80. In the next compound in this series, the terminal piperazine ring was replaced with phenyl with the expectation of achieving increased lipophilicity and perhaps enhanced binding, as was observed in the quinazolinone series (data not shown). Compound **10** (Table I) did not, however, show improved in vitro IC_{50} against cells as compared to **9**. The low solubility of **10** prevented reliable determination of its K_i against *E. coli* TS; against human TS, the K_i was equivalent to that for **9**.

The obvious need to redesign the hydrogen-bonding interaction between inhibitor and protein and thereby to allow restoration of the displaced water 430 led to the replacement of the carbonyl group of the lactam with an amino group (compound **11**, Table I). This would ideally allow the ligand to approach Ala263 more closely by virtue of hydrogen-bond formation and to accommodate a water molecule in the 430-position. An additional expectation concerning the amino group was that either by protonation or tautomerism, a hydrogen attached to the ring nitrogen could donate a hydrogen bond to Asp169 while the exocyclic amino or imino group could still make one hydrogen bond to the restored water 430 and make an additional hydrogen bond, if in the amino tautomer or if protonated, to the backbone carbonyl of Ala263. The question of tautomeric preference in **11** was addressed by combined quantum mechanics and free energy perturbation methods,[26] and the results of the calculations indicate that the imino and amino tautomers are comparable in energy. No pK_a data for ring systems of this kind have been reported and thus the only way to address this point was by synthesizing the compound. Following synthesis, the K_is against human and *E. coli* TS were found to be 31 nM and 1.5 μM, respectively. We have determined the pK_a of **11** to be 8.0,[27] which is consistent with its being substantially protonated when bound in the active site of TS. The crystal structure was determined (Figure 6) and careful analysis of the electron density showed that water 430 had reappeared and that the separation (2.7 Å) and geometry between the carbonyl of Ala263 and the exocyclic amino group nitrogen was consistent with hydrogen-bond formation.

(26) (a) Weiner, S. J.; Kollman, P. A.; Case, D. A.; Singh, U. C.; Ghio, C.; Alagona, G.; Profeta, S.; Weiner, P. *J. Am. Chem. Soc.* **1984**, *106*, 765. (b) Singh, U. C.; Weiner, P. K.; Caldwell, J. K.; Kollmann, P. A. AMBER (UCSF) Version 3.0, 1986. (c) Frisch, M. J.; Head-Gordon, M.; Schlegel, H. B.; Raghavachari, K.; Binkley, J. S.; Gonzalez, C.; Defrees, D. J.; Fox, D. J.; Whiteside, R. A.; Seeger, R.; Melius, C. F.; Baker, J.; Martin, R.; Kahn, L. R.; Stewart, J. J. P.; Fluder, E. M.; Topiol, S.; Pople, J. A. Gaussian, Inc., Pittsburgh, PA, 1988.

(27) Potentiometric titrations were performed at 25 °C as described by Albert and Serjeant (Albert, A.; Serjeant, E. P. *The Determination of Ionization Constants. A Laboratory Manual*, 3rd ed.; Chapman and Hall: New York, 1984.) in *N*,*N*-dimethylformamide:H_2O (67:33).

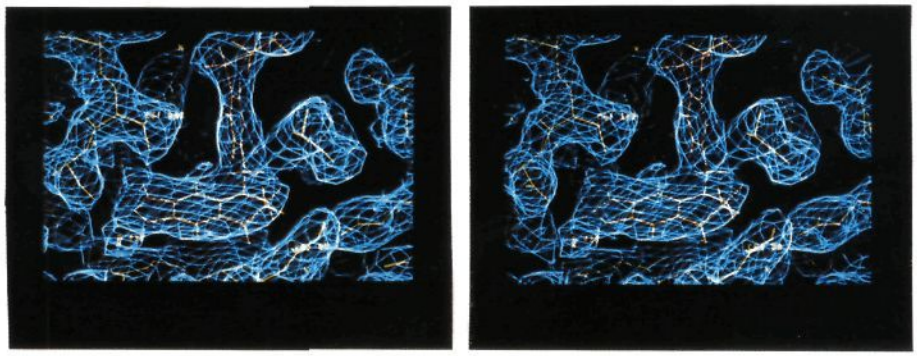

Figure 7. Electron density for the active site of an *E. coli* TS ternary complex containing FdUMP and compound **12**. The map is calculated at 2.5-Å resolution using coefficients $(2F_{der} - F_{par})e^{i\alpha\ par}$ where F_{der} and F_{par} refer to observed structure factor amplitudes for ternary complexes with compounds **12** and **1**, respectively, and α_{par} is a calculated phase for the latter complex based on our current refine model.[18]

As shown in Table I, each successive compound, except **10**, in this series is a better inhibitor against both *E. coli* and human enzymes. This is consistent with the broad similarities of the two active sites as expected from sequence homology and knowledge of the *E. coli* TS structure. This particular family of inhibitors does, however, show a consistent preference for binding to the human enzyme sometimes by as much as a factor of 50. Although we do not yet have any structural data on the human enzyme complexed with inhibitors in this series, our current explanation for this selectivity is as follows. The most striking difference between the *E. coli* and human enzymes deep in the active site are the residue changes Val262 to Met (311 in human) and Trp83 to Asn (112 in human). For the *E. coli* structure, this is known to be the area where the naphthalene ring binds. It is believed that in going from a Trp in *E. coli* to an Asn in the human, this area becomes somewhat larger and, therefore, accommodates the large naphthalene ring better.

The inhibition of cellular growth displayed by 8–11 (Table I) increased significantly through the series with compound **11** exhibiting an IC_{50} of 0.38 μM against the L1210 line. Some reversal of this inhibition by thymidine was observed only for the tightest binding inhibitor, compound **11**.[28] This suggests that these molecules may interact with additional receptors which contribute significantly to the inhibitory effects and that ligands with greater specificity for TS may be required.

(b) Development of Tetrahydroquinoline-Based Lead Compounds. The design of a second series of novel lead compounds started with an analysis of the hydrogen-bonding requirements of residues deep in the active site. The intent was to position a functional group so that it could both donate a hydrogen bond to Asp169 and accept a hydrogen bond from water 430. Initially, an imidazole ring was modeled into this part of the active site. Since the narrow hydrophobic cleft between the substrate analogue 5-fluorodeoxyuridylate and the surface created by Val262 and Trp83 could easily accommodate a second aromatic ring, this led to the modeling of a benzimidazole. Beyond the benzimidazole, the active site widens considerably before turning the corner toward Phe176. The GRID program predicts strong affinity for a methyl probe in this large hydrophobic pocket and this led to the idea of the addition of a saturated ring, reminiscent of the reduced cofactor. A 1,2,3,4-tetrahydroquinoline ring system, the aromatic ring of which overlayed the benzene ring of the benzimidazole, was therefore modeled, with the saturated ring filling the wider portion of the active site. Additional groups could be added to the nitrogen of the tetrahydroquinoline ring to pick up hydrophobic interaction with Phe176 and other side chains comprising the entrance to the active site. In common with the previous naphthostyril series, a benzyl group substituted at the para position with a sulfonyl piperazine when added to this nitrogen occupied the remaining space in the active site and was expected to confer water solubility. Conformational analysis of the substituted tetrahydroquinoline system using Gaussian 88 and semiempirical calculations followed by modeling experiments revealed puckered conformations of similar energy (within 1 kcal/mol), all of which could be accommodated readily by the protein in this region of the active site.

Compound **12** (Table I) was synthesized and found to have K_is of 4.9 and 7.7 μM against *E. coli* and human TS, respectively, and this established the linear tricyclic system as a novel lead. Figure 7 shows the fit of protein and ligand atoms to electron density for the active site region of *E. coli* TS complexed with **12**. A neck of continuous density between N1 of the ligand and water 430 and also between N3 of the ligand and Asp169 coupled with the binding geometry are consistent with hydrogen-bonding interactions. Figure 8 shows the crystal structure of the *E. coli* TS complex with the tricyclic portion of **12** and reveals that the molecule bound largely as modeled. There was a minor rotation with respect to the modeled conformation of the phenyl ring off of the tetrahydroquinoline nitrogen (a torsion between the benzyl carbon and the phenyl ring). This difference between modeled and bound conformations, which ranges from 20° to 30°, has been observed in each of the complex structures described here and in other complexes in this series. In every case, the phenyl ring moved away from an edge-on interaction with Phe176 (as seen in **1** and **5**) to one that is more parallel, being sandwiched between Phe176 and Leu172. This represents an alternative mode of binding for the right-hand portion in this series, relative to the quinazoline-based inhibitors. As anticipated, N3 of the benzimidazole system in compound **12** donates a hydrogen bond to Asp169 as inferred from the distance (2.9 Å) and geometries observed in the crystal structure. The saturated ring of the tetrahydroquinoline ring was well accommodated by the protein, making close van der Waals contact with Ile79 and Trp80. The binding geometry of the tricyclic portion of **12** indicated that additional hydrogen bonding to the backbone carbonyl oxygen of Ala263 and contact with the protein C-terminus might be achieved by positioning an amino group at the

(28) A derivative of **11** has shown much increased reversal of inhibition of cell growth in the presence of thymidine (Varney, M. D.; Deal, J. G.; Bartlett, C. A.; Morse, C. A.; Webber, S., unpublished results).

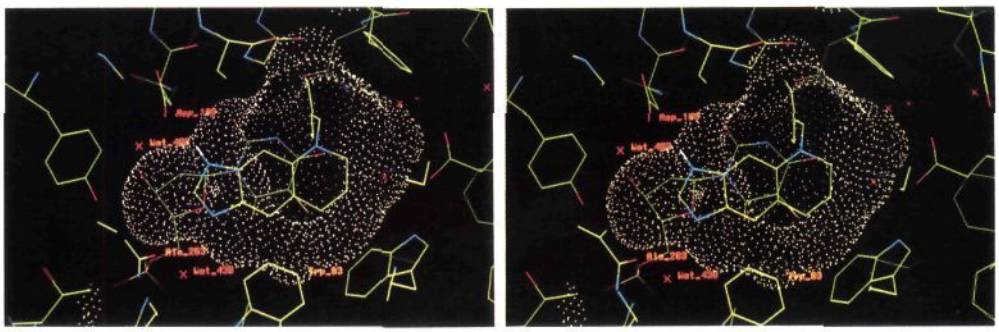

Figure 8. Stereo drawing showing the structure of **12** complexed with *E. coli* TS. The tricyclic portion of the inhibitor is shown indicating the interactions with the side chains of Trp80 and Trp83. The vacant space off the 2-position of the benzimidazole is apparent from the protein solvent accessible surface.

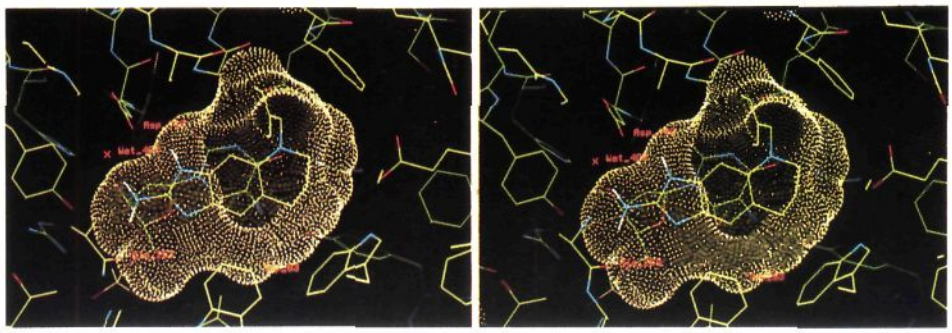

Figure 9. Stereo drawing showing the structure of **14** complexed with *E. coli* TS. The tricyclic portion of the inhibitor is shown indicating the inferred hydrogen-bonding interactions with the side chain of Asp169, water 402, and the backbone carbonyl of Ala263. The space vacated by water 430 is clearly visible within the protein solvent accessible surface.

2-position of the imidazole ring. The modeled position of this amino group was virtually identical with that of the 2-amino group in the classical quinazoline series (exemplified by **1**) wherein that substituent was known to increase binding 8-fold.[29]

Amino analogue **13** (Table I) was synthesized and showed improved binding, relative to **12**, by a factor of 35 against *E. coli* TS and by a factor of 120 against human TS. When, in a subsequent molecule (**14**, Table I), the piperazine ring was also replaced by phenyl, the K_is dropped to 43 and 31 nM against *E. coli* and human enzymes. Detailed analysis of the crystal structures of **13** and **14** indicated that the tricycle bound essentially as modeled and in about the same position as compound **12**. Figure 9 shows the bound conformation of the tricyclic portion of compound **14**. The terminal amino group makes a hydrogen bond to the carbonyl of Ala263 with the carbonyl oxygen being slightly out of the plane of the imidazole ring. A marked difference between the 2-amino-substituted inhibitors in this series (as exemplified by **14**) and compound **12** was the disappearance of water molecule 430 in the complexes containing 2-amino derivatives ascertained by analysis of both the $2F_o - F_c$ and F_o difference electron density maps. The significant increase in binding affinity to the human enzyme in going from the 2-H (120-fold) or 2-methyl[30] (14-fold) to the 2-amino benzimidazole is in direct contrast with the modest difference (8-fold for hydrogen[29] and 2-fold for methyl[11]) observed in the classical quinazoline series despite their virtually identical position in the active site. It is likely that both the enhancement in binding and the consistent expulsion of water molecule 430 are a result of the 2,5-diaminobenzimidazole system being protonated at N1 when bound in the active site. We have determined the pK_a of this tricyclic ring system to be 8.2, which is consistent with this interpretation.[27,31] In addition, the electron density for the tetrahydroquinoline portion of the tricycle in compound **12** is more diffuse than that of the 2-amino derivatives, suggesting that the position of compound **12** is less well-defined in this region, which could be related to its weaker binding.

Growth inhibition of L1210 cells increased 10-fold (IC_{50} values dropping from 20 to 2 μM) with the development of this series (Table I). The similarity in inhibition between compounds **13** and **14** did not directly parallel the two-fold increase in affinity for TS although the underlying basis for the observed cytotoxicity may differ for the two compounds since a slight reversal effect with thymidine

(29) Jones, T. R.; Thornton, T. J.; Flinn, A.; Jackman, A. L.; Newell, D. R.; Calvert, A. H. *J. Med. Chem.* **1989**, *32*, 847.

(30) A related 2-methyl derivative of compound **14** has been prepared (Reich, S. J.; Fuhry, M. M., unpublished results) and has a K_i of 0.43 μM against human and 1.3 μM against *E. coli* TS (Ward, R.; Welsh, K. M., unpublished results).

(31) Preston, P. N. *The Chemistry of Heterocyclic Compounds, 40 Wiley and Sons: New York, 1981; Part I.*
(32) Lomax, M. I. S.; Greenberg, G. R. *J. Biol. Chem.* **1967**, *242*, 109.
(33) Cleland, W. W. *Biochim. Biophys. Acta* **1963**, *67*, 173.
(34) Perrella, F. W. EZ-FIT, Perrella Scientific, Springfield, PA., 1989.
(35) Dixon, M.; Webb, E. C. *Enzymes*, 3rd ed.; Academic Press: New York, 1979; pp 334–341.
(36) Jackson, R. C.; Jackman, A. L.; Calvert, A. H. *Biochem. Pharmacol.* **1983**, *32*, 3783.
(37) Alley, M. C.; Scuderio, D. A.; Monks, A.; Hursey, M. L.; Czerwinski, M. J.; Fine, D. L.; Abbott, B. J.; Mayo, J. G.; Schoemaker, R. H.; Boyd, M. R. *Cancer Res.* **1988**, *48*, 589.
(38) MTT is 3-(4,5-dimethylthiazol-2-yl)-2,5-diphenyltetrazolium bromide.
(39) Mosmann, T. *J. Immunol. Methods* **1983**, *65*, 55.
(40) (a) Connolly, M. L. *J. Appl. Crystallogr.* **1983**, *16*, 548. (b) Connolly, M. L. *J. Am. Chem. Soc.* **1985**, *107*, 1118.

was seen with **14** but not with **13**. The reduction in K_i achieved by the design modifications between these two derivatives may have led to more directed targeting in vitro.

Conclusions

We have used an iterative cyclic process to develop three substantially different structural classes of molecules into potent inhibitors of the enzyme *E. coli* thymidylate synthase. The development of these inhibitors has progressed to the point where a compound from each of these classes can be considered to be a drug lead. From the case histories reported in this paper, we can make the following general observations.

Crystallographic analysis of ligand binding is a useful and important tool for ligand design. It can be used experimentally to deduce binding geometries for new lead compounds, to reveal subtle differences in binding between successive members of a series of compounds, and to reveal conformational changes in the receptor that accompany binding. This knowledge can then be exploited during subsequent design.

To be optimally useful, the receptor crystal structures must be refined at high resolution. In terms of free energy, the difference between micromolar and nanomolar binding constants is not large (ca. 4 kcal/mol). High-resolution receptor structures provide a better opportunity for observing subtle but perhaps significant differences, for example in the binding of water molecules, that may influence subsequent design. The high-resolution receptor structures, on which the design efforts described in this paper were based, allowed us to proceed from micromolar range inhibitors to nanomolar range inhibitors with minimal chemical synthesis. Indeed, only three compounds were required in the best case.

If a putative favorable binding geometry between ligand and receptor can be modeled with the ligand in a low-energy conformation, then both the desired binding geometry and a ligand conformation close to the modeled conformation will most likely be observed in the ligand–receptor crystal structure.

The methodology can provide a variety of chemically distinct lead compounds that have comparable inhibition constants but display different properties in cultured cells and presumably in whole animals.

When analyzing differences in binding between inhibitors in a series and correlating them with in vitro inhibition constants, several factors are not currently considered in any detail. Perhaps the most important of these is the free energy difference associated with ligand and protein desolvation in their going from free to bound form. This underscores the view that the crystallographic analysis of ligand binding is only one component, albeit an important one, in the design and development of drug leads. Perhaps for these reasons, it has been easier, in our experience, to discover novel lead compounds with potencies in the micromolar range by satisfying evident nonpolar and electrostatic requirements of the active site than it has been to elaborate these leads into nanomolar inhibitors with a small number of iterations. The subtle and less tangible changes accompanying small functional group substitutions, not always interpretable from the structural data, may play a more significant role at this level.

It has also emerged from this work that a highly homologous surrogate receptor can be successfully used to discover and optimize leads. Clearly this is not a generic principle, as many instances of species selectivity at the inhibitor–receptor level exist, but provided that the structure of the receptor from one species is known, we have shown that differences in three-dimensional structure can be estimated and exploited from known primary sequence heterology.

It is encouraging that significant in vitro inhibition of cellular growth was observed for most of the compounds described and that the IC_{50} values generally follow the same trend as the human K_is. The interpretation of the data obtained for the more novel compounds may, however, be complex. A low K_i for any class of inhibitor does not necessarily lead to exclusive targeting of TS—a factor that becomes more significant in in vivo tests when binding to additional cellular components may lead to undesired toxic side effects. A potential advantage of the approach described in this work is that it yields a variety of chemically distinct lead compounds with comparable inhibition constants, but which are likely to display inherently different pharmacological and toxicity profiles. The analysis of receptor targeting in vivo and in vitro continues to be a focus in the development of clinical candidates from these and other novel structural series.

The superiority of the strategy described for the discovery of drugs over existing methods remains to be investigated. We have presented evidence that three substantially different structural classes of molecules have been either discovered or elaborated or both using the crystal structure of a pharmacologically significant receptor. In the course of this work, we have generated a further four structurally distinct novel leads with K_is ≤ 1 μM (data not shown). The three leads described have been improved in vitro by between 100- and 1000-fold in a short series of iterative steps involving crystallographic analysis without any prior knowledge of the SAR. These data strongly suggest that the methodology is good for generating drug leads with nanomolar potencies at the receptor level. Insofar as drug discovery depends on the number and structural diversity of drug leads, our data support the view that drug discovery will be speeded by judicious application of these techniques.

Acknowledgment. We thank Peter Johnson, Dr. David Henry, and the staff of Agouron Pharmaceuticals, Inc., for their support and encouragement of this work. Numerous colleagues at Agouron Pharmaceuticals, notably Bob Almassy, Dom Zichi, and Steve Jordan, have contributed ideas to the work described and we thank them. We thank Dottie Olson and Lisa Kingery for their expert assistance in preparing the manuscript.